Mon. Not. R. Astron. Soc. **000**, 1–9 (2012) Printed 23 January 2013 (MN LATEX style file v2.2)

Light curve analysis and orbital period change of the extreme mass-ratio overcontact binary AW CrB

Eric Broens[1⋆]
[1] *Vereniging Voor Sterrenkunde, Belgium*

Accepted 2013 January 17. Received 2013 January 16; in original form 2012 April 17

ABSTRACT
Extreme mass-ratio contact binaries with a high degree of overcontact may be in the late evolutionary stages of the contact phase. Detailed photometric analyses and orbital period studies of those systems can provide invaluable information for the coalescence scenario of close binary systems, as recently observed in V1309 Sco. In this paper the first light curve analysis and period study for the totally eclipsing contact binary AW CrB is presented. The VR_cI_c CCD photometric light curves are analysed by means of the WD code. The asymmetry of the light curves is modelled by a cool star spot on the primary component. It is shown that AW CrB has a high degree of overcontact $f = 75$ % and an extreme mass-ratio of $q = 0.10$, placing it among the few contact binaries with the lowest known mass-ratios. The mean density of the primary component suggest that it has evolved away from the ZAMS.
Eighty-four times of minimum light are reported, derived from observations available in public archives, the literature, and the observations presented in this paper. The orbital period study shows a continuously increasing period, at a rate of $\mathrm{d}P/\mathrm{d}t = 3.58 \times 10^{-7}\ d\ yr^{-1}$, suggesting a mass transfer from the secondary component to the primary one, implying a further decreasing mass-ratio.

Key words: binaries: close binaries: eclipsing – stars: individual (AW CrB)

1 INTRODUCTION

The evolution of W UMa-type binary stars is still not well understood. The traditional view for the origin of these contact binaries is that they are formed from detached cool binaries with initial orbital periods of a few days. By a combination of evolutionary expansion of both components and angular momentum loss arising from the magnetic stellar wind, a contact binary is formed. Model calculations suggest that these binary systems ultimately coalesce into single stars and may be progenitors of the poorly understood blue straggler and FK Com-type stars (e.g. Rasio 1995; Stępień 2006, 2011). It was recently demonstrated that the eruption of V1309 Sco was the result of a merger of the components of a cool contact binary (Tylenda et al. 2011). Extreme mass-ratio contact binaries with a high degree of overcontact may be in the late evolutionary stages of the contact phase. Detailed photometric analyses and orbital period studies of those systems can provide invaluable information for the evolution and coalescence scenario of these binary systems.

The variability of AW CrB was discovered in the course of the ROTSE-I experiment, and classified as a δ Scuti-type star with a period of $0^{\mathrm{d}}.180465$d (Akerlof et al. 2000). The variable identification, period determination, and type classification were conducted by automatic algorithms. Jin et al. (2003) found, from visual inspections of the light curves of the ROTSE-I δ Scuti stars, that several of these stars were misclassified. In order to re-classify some of these stars, they started a multiband photometric CCD observing programme for 20 of the 91 stars classified as δ Scuti star in the initial ROTSE-I variable star catalogue. From their single night observations they found AW CrB to be a W UMa-type star with an amplitude of about 0.3 mag. By combining the ROTSE-I data with their observations, they derived a period of $0^{\mathrm{d}}.360920$. Their light curve of AW CrB displays total eclipses making this star very suitable for a photometric study. The mass-ratio of W UMa-type stars exhibiting total eclipses can be accurately determined from photometric observations (Terrell & Wilson 2005). The long total eclipses of AW CrB, lasting about 10 per cent of the orbital period, in combination with the small amplitude suggest a low mass-ratio making this star particularly interesting.

The position of AW CrB furthermore coincides with the *ROSAT* X-ray source 1RXS J161520.0+354218 (Geske, Gettel & McKay 2006) indicating chromospheric activity. Since no light curve model has been published yet, new photometric VR_cI_c CCD observations were obtained.

⋆ E-mail: eric.broens@skynet.be

In this paper the photometric analysis of these observations, using the Wilson-Devinney (WD) code (Wilson & Devinney 1971, 1972; Wilson 1979, 1994), are presented together with a period study. For the orbital period study also the observations published by Jin et al. (2003) and photometric data obtained by the ROTSE and WASP robotic telescopes are used.

2 OBSERVATIONS

AW CrB was observed on eight nights in 2011 from a private observatory located near the town of Mol, Belgium, at an altitude of about 40 meter above sea-level. The images were acquired using a 20-cm Celestron Schmidt-Cassegrain telescope, equipped with a SBIG ST-7XMEI CCD camera, and VR_cI_c filters which are close to the standard Johnson-Cousins system. The use of a focal reducer yields a field of view of 16.8′ by 11.2′ and a plate scale of 1.32″/pixel. The operating temperature of the CCD was kept constant at a temperature about 30 degrees below the ambient temperature. For most of the nights the operating temperature was kept constant at -20°C. On the second night the CCD was cooled to -25°C and on the last two nights to -15°C. The observations were made under good to excellent sky conditions, i.e. no sudden drops in the instrumental magnitudes, e.g. due to cirrus clouds, have been observed. However, on JD 2455672 the observations had to be stopped early due to deteriorating weather conditions.

The integration time for each image was 60 *s*. By using the CCD camera's additional autoguider chip, the stars were kept on approximately the same pixels during an observing session. The FWHM of the stellar images was typically around 4 pixels, occasionally increasing to more than 5 pixels partly due to a focus drift caused by the decreasing ambient temperature.

The images were processed with dark removal and flat-field correction using the imred packages in IRAF[1]. Twilight flat-field images were obtained on all but two nights on which the flat-fields were obtained from a diffuse reflector indirectly illuminated by an incandescent lamp. Vignetting is evident in the flat-field images with about 5 to 10 per cent loss of intensity at the very corners of the image. The variable, comparison, and check star are well located around the central area of the image which is not affected by the vignetting.

Differential aperture photometry was performed using the digiphot/apphot package in IRAF. GSC 2586-1883 and GSC 2586-1807 were chosen as the comparison and the check star respectively. The coordinates, V magnitude, and colours of AW CrB, the comparison, and the check star are listed in Table 1. The magnitude and colours for the comparison and check star are taken from the AAVSO Photometric All Sky Survey (APASS), which is conducted in five filters: Johnson B and V, plus Sloan g', r' and i' (Henden et al. 2012). Using the equations from Jester et al. (2005), the APASS Sloan magnitudes of the comparison and check star have been transformed to $V - R_c$ and $R_c - I_c$ colours in order to transform the differential observations of AW CrB to the standard Johnson-Cousins system. The comparison star was close enough to the variable that extinction differences were negligible. The observations were made at airmasses smaller than 1.90.

[1] IRAF is distributed by the National Optical Astronomy Observatories, which are operated by the Association of Universities for Research in Astronomy, Inc., under cooperative agreement with the National Science Foundation.

Table 2. Observation log.

Julian day	Number of hours	Number of data points V	R_c	I_c
2455661	6.7	101	101	101
2455664	6.3	92	91	91
2455672	4.6	59	54	54
2455676	6.9	104	104	104
2455677	7.1	108	107	107
2455685	3.9	64	65	65
2455714	5.2	76	75	75
2455715	4.8	72	70	70
Total	45.5	676	667	667

Depending on the airmass and the sky conditions, the integration time of 60 *s* results in a signal-to-noise ratio for the V filter between 251 and 521 for the variable, between 215 and 451 for the comparison star, and between 332 and 531 for the check star. For the R_c and I_c filters the signal-to-noise ratio is somewhat higher. An estimate of the uncertainty of the CCD photometry was obtained from the standard deviation of the differential light curve between comparison and check star, viz. 0.01 magnitude in all filters. Since the photometric error is dominated by the fainter star, in this case the comparison star, the above figure is a good estimate for the uncertainty of the variable minus comparison star light curve (e.g. Howell, Warnock & Mitchell (1988)). About 46 *h* of CCD photometry was secured in each passband covering all orbital phases of AW CrB several times. The complete observation log is given in Table 2 and phased light curves are shown in Figure 1. All observations are available from the AAVSO International Database[2] or upon request from the author.

3 ECLIPSE TIMINGS AND ORBITAL PERIOD STUDY

Up to now no times of minimum light had been published yet. From the observations reported in the present paper two timings of primary minimum and five timings of secondary minimum were determined using the Kwee & van Woerden (1956) method. This method was also applied on the primary and secondary minimum observed by Jin et al. (2003) and to the publicly available photometry from the WASP project (Butters et al. 2010). To calculate the time of minimum light from the data of the Northern Sky Variability Survey (NSVS) (Wozniak et al. 2004), the observations were first phased before applying the Kwee & van Woerden method. All timings of minimum light, spanning almost 12 years or about 12000 orbital revolutions, are listed in Table 3. The timings from our observations and from Jin et al.

[2] http://www.aavso.org

Table 1. The coordinates, V magnitude and colours of AW CrB, comparison and check star.

Star	α(2000.0)	δ(2000.0)	V	$V-R_c$	R_c-I_c
AW CrB	$16^h15^m20\overset{s}{.}2$	$+35°42'26\overset{''}{.}2$	10.97	0.30	0.31
GSC 2586-1883 (comparison)	$16^h15^m21\overset{s}{.}4$	$+35°50'19\overset{''}{.}0$	11.73	0.49	0.46
GSC 2586-1807 (check)	$16^h14^m56\overset{s}{.}1$	$+35°50'09\overset{''}{.}3$	10.43	0.57	0.53

For AW CrB the magnitude and colours at maximum light are listed, obtained from the observations presented in this paper. The magnitude and colours for the comparison and check star are taken from the AAVSO Photometric All Sky Survey (APASS).

Table 3. Times of minima of AW CrB.

Epoch	HJD 2 400 000+	data*	Epoch	HJD 2 400 000+	data*	Epoch	HJD 2 400 000+	data*
-6730.5	51401.5390 ± 0.0050	(1)	1179.5	54256.5316 ± 0.0008	(3)	2058.0	54573.6121 ± 0.0007	(3)
-6730.0	51401.7197 ± 0.0050	(1)	1182.0	54257.4317 ± 0.0016	(3)	2063.5	54575.5974 ± 0.0011	(3)
-3908.5	52420.0945 ± 0.0003	(2)	1193.5	54261.5837 ± 0.0004	(3)	2072.0	54578.6654 ± 0.0007	(3)
-3908.0	52420.2749 ± 0.0003	(2)	1196.0	54262.4863 ± 0.0005	(3)	2074.5	54579.5666 ± 0.0009	(3)
-0.5	53830.6248 ± 0.0013	(3)	1199.0	54263.5695 ± 0.0008	(3)	2077.5	54580.6502 ± 0.0009	(3)
5.0	53832.6097 ± 0.0003	(3)	1204.5	54265.5544 ± 0.0007	(3)	2088.5	54584.6208 ± 0.0010	(3)
146.0	53883.5033 ± 0.0021	(3)	1207.0	54266.4572 ± 0.0006	(3)	2094.0	54586.6078 ± 0.0006	(3)
997.0	54190.6585 ± 0.0005	(3)	1210.0	54267.5399 ± 0.0005	(3)	2127.0	54598.5157 ± 0.0011	(3)
1030.0	54202.5717 ± 0.0019	(3)	1212.5	54268.4422 ± 0.0008	(3)	2152.0	54607.5401 ± 0.0008	(3)
1033.0	54203.6534 ± 0.0008	(3)	1215.5	54269.5246 ± 0.0006	(3)	2157.5	54609.5275 ± 0.0022	(3)
1060.5	54213.5780 ± 0.0011	(3)	1218.0	54270.4269 ± 0.0005	(3)	2171.5	54614.5776 ± 0.0019	(3)
1066.0	54215.5646 ± 0.0008	(3)	1221.0	54271.5098 ± 0.0007	(3)	2188.0	54620.5367 ± 0.0010	(3)
1069.0	54216.6478 ± 0.0006	(3)	1226.5	54273.4943 ± 0.0011	(3)	2193.5	54622.5205 ± 0.0004	(3)
1074.5	54218.6327 ± 0.0012	(3)	1229.5	54274.5790 ± 0.0030	(3)	2218.5	54631.5396 ± 0.0011	(3)
1088.0	54223.5029 ± 0.0041	(3)	1232.0	54275.4787 ± 0.0010	(3)	2221.0	54632.4453 ± 0.0004	(3)
1091.0	54224.5872 ± 0.0019	(3)	1235.0	54276.5620 ± 0.0007	(3)	2235.0	54637.4993 ± 0.0009	(3)
1094.0	54225.6701 ± 0.0031	(3)	1240.5	54278.5481 ± 0.0012	(3)	2246.0	54641.4702 ± 0.0006	(3)
1099.5	54227.6553 ± 0.0014	(3)	1243.0	54279.4483 ± 0.0010	(3)	2271.0	54650.4924 ± 0.0010	(3)
1102.0	54228.5572 ± 0.0007	(3)	1248.5	54281.4339 ± 0.0011	(3)	2276.5	54652.4767 ± 0.0013	(3)
1107.5	54230.5426 ± 0.0007	(3)	1251.5	54282.5182 ± 0.0009	(3)	2287.5	54656.4483 ± 0.0007	(3)
1110.5	54231.6254 ± 0.0007	(3)	1257.0	54284.5026 ± 0.0004	(3)	2329.0	54671.4262 ± 0.0009	(3)
1116.0	54233.6118 ± 0.0010	(3)	1262.5	54286.4873 ± 0.0010	(3)	5072.0	55661.4760 ± 0.0003	(4)
1121.5	54235.5970 ± 0.0006	(3)	1268.0	54288.4732 ± 0.0004	(3)	5080.5	55664.5432 ± 0.0002	(4)
1124.0	54236.4998 ± 0.0009	(3)	1273.5	54290.4579 ± 0.0009	(3)	5102.5	55672.4850 ± 0.0006	(4)
1160.0	54249.4904 ± 0.0011	(3)	1279.0	54292.4442 ± 0.0005	(3)	5113.5	55676.4537 ± 0.0003	(4)
1163.0	54250.5731 ± 0.0007	(3)	1287.5	54295.5114 ± 0.0011	(3)	5116.5	55677.5359 ± 0.0003	(4)
1165.5	54251.4793 ± 0.0010	(3)	2016.5	54558.6344 ± 0.0008	(3)	5219.0	55714.5343 ± 0.0002	(4)
1168.5	54252.5618 ± 0.0013	(3)	2052.5	54571.6249 ± 0.0031	(3)	5221.5	55715.4363 ± 0.0002	(4)

*data: (1) NSVS (Wozniak et al. 2004), (2) Jin et al. (2003), (3) WASP (Butters et al. 2010), (4) this paper.
For minima observed in more than one passband the weighted mean of the timings in those passbands is listed.

(2003) are weighted means from the timings of minimum light in the respectively 3 and 2 observation bandpasses.

From the timings in Table 3 the following linear least-squares ephemeris is obtained:

$$HJD\ Min\ I = 2453830.8080(3) + 0\overset{d}{.}3609353(1) \times E \qquad (1)$$

The $O-C$ residuals calculated with these ephemeris are plotted in Figure 2. The estimated errors of the minimum light timings, also calculated according Kwee & van Woerden (1956), cannot account for the scatter in the $O-C$ diagram. These formal errors often underestimate the real error, due in part to random errors but there could also be biases arising from systematic differences in the shape of the descending and ascending branches of the eclipse light curve. Nevertheless, the $O-C$ diagram indicates an increase of the orbital period. The form of the period change is unclear due to the large gaps between the groups of minimum light timings and the relative short time span of the observations. A sudden period increase and a constant period increase are considered.

If the period change is a sudden increase then with the data for $E \leqq 146$ a least-squares linear fit yields the ephemeris

$$HJD\ Min\ I = 2453830.8056(4) + 0\overset{d}{.}3609341(1) \times E \qquad (2)$$

With the data in the range of $-0.5 \leqq E \leqq 5221.5$ we obtain

$$HJD\ Min\ I = 2453830.8058(2) + 0\overset{d}{.}3609364(1) \times E \qquad (3)$$

With these equations a sudden period increase of $\Delta P = 2.3 \times 10^{-6}\ d$ or $0.2\ s$ is estimated to have occured around $2005 - 2007$. Figure 3 shows the phase diagram constructed with equation (3) for the WASP data (solid line),

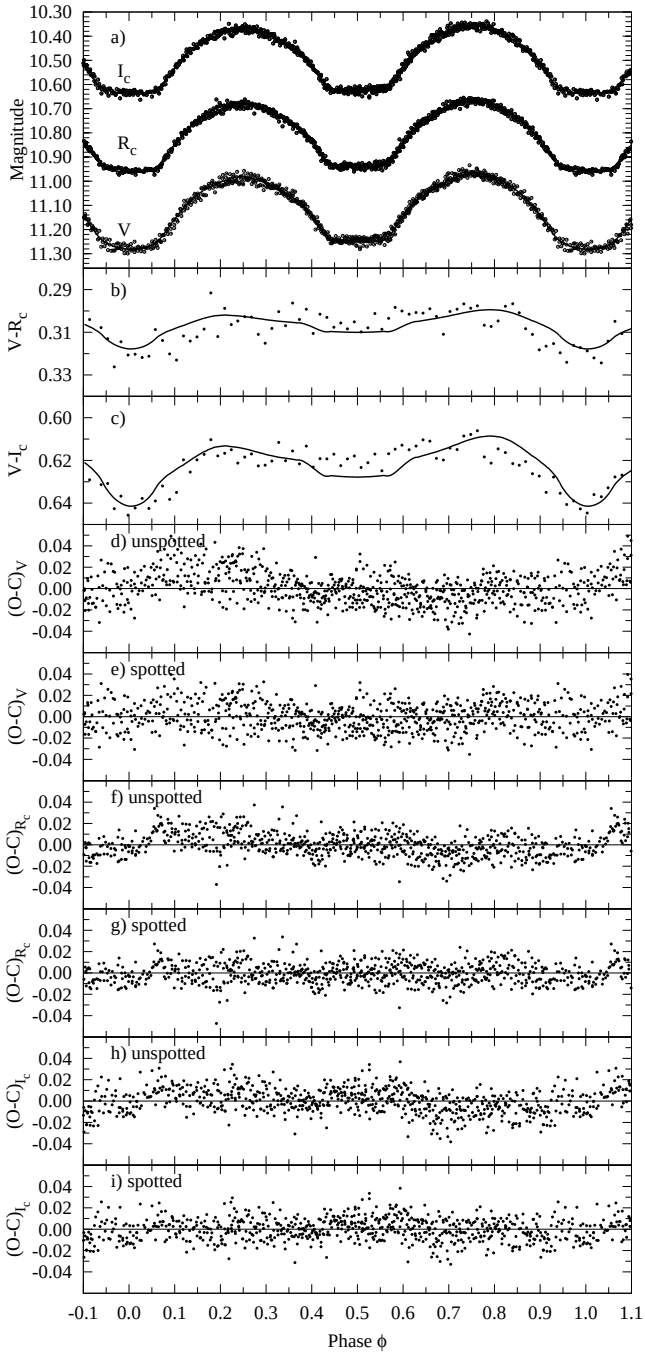

Figure 1. VR_cI_c light curves (a) and colour curves (b and c) of AW CrB, the solid line is the synthetical light curve of the model with a cool spot on the primary. The dots in the colour curves represent mean values calculated in a phase bins of $\phi = 0.015$. The lower panels display the residuals of the unspotted and spotted model fits for the V (d and e), R_c (f and g) and I_c passband (h and i) respectively.

the R_c observations from this paper (circles), the Jin et al. (2003) I band observations (filled squares), and the NSVS data (triangles). The WASP, NSVS, and Jin et al. (2003) data were shifted in magnitude to fit the observations presented in this paper. For the sake of clarity averaged WASP observations are plotted. The phase diagram demonstrates clearly the phase shift of the NSVS and Jin et al. (2003)

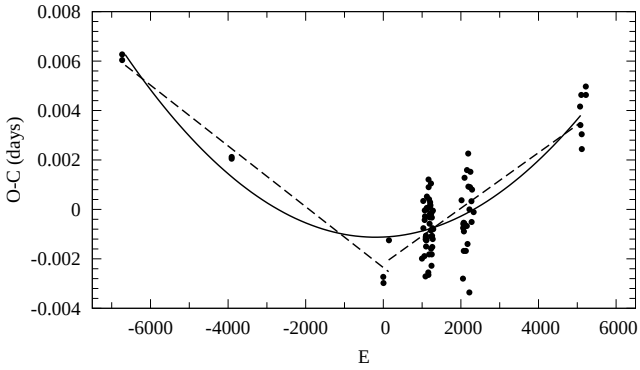

Figure 2. $O - C$ diagram of AW CrB. Dashed lines refer to a sudden period increase and solid line to a continuous period increase.

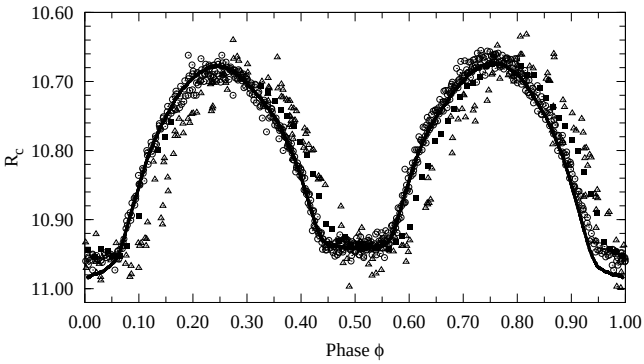

Figure 3. Phase diagram of AW CrB constructed using the ephemeris in eq. (3). The solid line represents averaged WASP observations. The circles, triangles, and filled squares are respectively the R_c observations presented in this paper, the NSVS observations, and the I band data from Jin et al. (2003). The observations were shifted in magnitude to fit the observations presented in this paper.

data with respect to the WASP data and the R_c observations from this paper due to the period change.

Assuming a constantly increasing period, a quadratic least-squares fit to the light time minima yields following ephemeris:

$$HJD\ Min\ I = 2453830.8069(2) + 0^{\rm d}.36093537(6) \times E + 1.8(1) \times 10^{-10} \times E^2 \quad (4)$$

From the quadratic term of equation (4), a continuous period increase rate of $\mathrm{d}P/\mathrm{d}t = 3.58 \times 10^{-7}\ d\ yr^{-1}$ or $0.03\ s\ yr^{-1}$ is derived. However, due to the short time span of the observations, a cyclic period variation cannot be ruled out.

The period analysis has been repeated using the timings of primary and secondary minimum separately. The results are not significantly different from those obtained with both the primary and secondary minima included in the analysis.

4 LIGHT CURVE ANALYSIS

The Wilson-Devinney (WD) method, as implemented in the software package PHOEBE version 0.31a (Prša & Zwitter 2005), was used to analyse our V, R_c, and I_c light curves

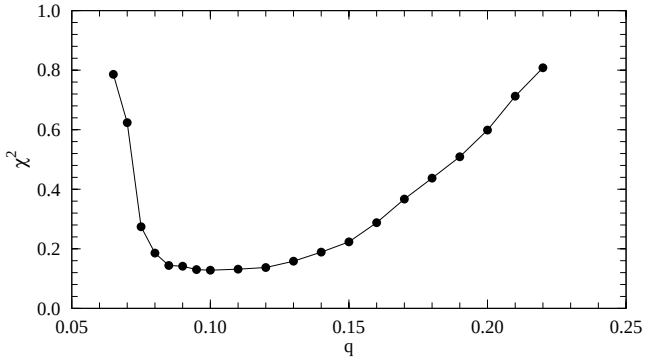

Figure 4. Total χ^2 for an unspotted model vs. a number of fixed mass-ratios q.

simultaneously. All individual data points were used in the analysis. Based on the colour indices $B-V = 0.505 \pm 0.024$, $V - R_c = 0.309 \pm 0.017$, $R_c - I_c = 0.286 \pm 0.005$, and interstellar reddening of $E(B-V) = 0.019$ published by Terrell, Gross & Cooney (2012) and the 2MASS colours $J - H = 0.210$, $H - K_s = 0.055$, the temperature of star 1 (the star eclipsed at primary minimum, i.e. phase $\phi = 0$) was fixed at $T_{\rm eff} = 6700$ K (Cox 2000). Based on the temperature, convective atmospheres are assumed. The bolometric albedos $A_1 = A_2 = 0.5$ (Rucinski 1969) and the gravity-darkening coefficients $g_1 = g_2 = 0.32$ (Lucy 1967), appropriate for convective envelopes, were assigned. The logarithmic limb-darkening law is used with coefficients adopted from van Hamme (1993) for a solar composition star. The analysis is performed in mode 3, which is appropriate for overcontact systems that are not in thermal contact. A q-search method was applied to determine the initial mass-ratio. For a range of discrete values of q, the adjustable parameters were: the orbital inclination i; the mean temperature of star 2, T_2; the monochromatic luminosities of star 1, L_1; and the dimensionless potential of star 1 ($\Omega_1 = \Omega_2$, for overcontact binaries). From Figure 4, it can be seen that the resulting chi-square value of the convergent solutions reached its minimum for $q = 0.10$. At this point the mass-ratio q, with initial value 0.10, was included in the set of the adjustable parameters. The mass-ratio converged to a value of $q = 0.0992 \pm 0.0004$ in the final solution, with a total $\chi^2 = 0.129$. The solution reveals a high degree of overcontact $f = (\Omega_{in} - \Omega)/(\Omega_{in} - \Omega_{out}) = 75\% \pm 3$. The photometric parameters are listed in Table 5 and the residuals of the fit are plotted in Figure 1 panels d, f, and h for the V, R_c, and I_c passband respectively. The errors given in this paper are the formal errors from the WD code and are known to be unrealistically small.

While the overall fit of the computed light curves is quite satisfactory, Figure 1 shows the maximum at phase $\phi = 0.25$ (Max I) slightly fainter than at phase $\phi = 0.75$ (Max II) by about 0.02, 0.01, and 0.01 mag in the V, R_c, and I_c bandpasses respectively. Table 4 lists the average magnitudes calculated in a phase interval of ± 0.02 around the maxima and minima, with the standard deviation in units of the last digit given between parentheses. The unequal light level between primary maximum and secondary maximum, the so-called O'Connell effect, is known in many eclipsing binaries. It is often explained as surface inhomogeneities on either or both components and modelled by placing circular dark or hot spots on the components.

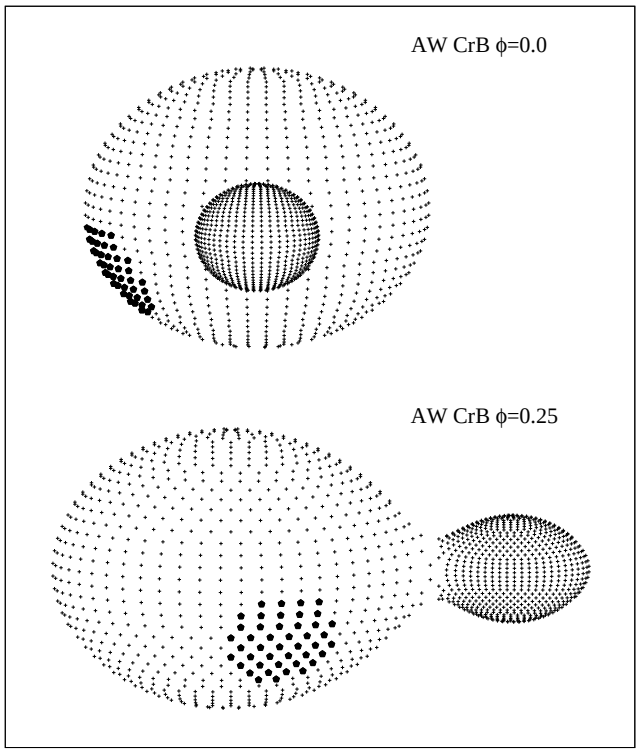

Figure 5. Geometrical representation of AW CrB at phases $\phi = 0.0$ and $\phi = 0.25$.

We assumed that either a hot spot or a cool spot was on star 1 or star 2. For these four combinations and with the parameters from the spotless solution fixed, the parameter space of colatitudes ϕ, longitudes θ, spot radius r_s, and temperature factor $T_s/T_\star$, with $T_\star$ being the local effective temperature of the surrounding photosphere, was explored using the phoebe-scripter. The best solution was found for a cool spot on the primary, with $T_s/T_\star = 0.96$, spot radius $r_s = 21^\circ$, colatitude $\phi = 114^\circ$, and longitude $\theta = 290^\circ$. Since a solution didn't converge with subsets of spot parameters made adjustable, these spot values were fixed while the higher mentioned set of star parameters was made adjustable again. This resulted in a solution with a total $\chi^2 = 0.104$. All parameters are listed in Table 5 and the fit of the computed light and colour curves is plotted in Figure 1 panels a, b, and c. The corresponding geometric structures at phases $\phi = 0.00$ and $\phi = 0.25$ are displayed in Figure 5. As shown by Maceroni & van't Veer (1993), spot determination by photometry alone is unreliable because of the non-uniqueness of photometric solutions for spotted W UMa-type binaries. The spot parameters listed in Table 5 are therefore only provisional. Since Pribulla & Rucinski (2008a) argue that perhaps all cool contact binaries are members of multiple systems, and a cyclic period variation cannot be ruled out, a third light contribution to the light curves has been investigated. The analysis however did not reveal a third light contamination. Mochnacki & Doughty (1972) have shown that the internal contact angle for a given mass-ratio q, and inclination i, is almost independent of the degree of overcontact f. The

Table 4. Average maximum and minimum magnitudes.

Filter	Max I $\phi = 0.25$	Max II $\phi = 0.75$	Min I $\phi = 0.0$	Min II $\phi = 0.50$
V	10.99(1)	10.97(1)	11.28(1)	11.25(1)
R_c	10.68(1)	10.67(1)	10.96(1)	10.94(1)
I_c	10.37(1)	10.36(1)	10.63(1)	10.62(1)

Table 5. Light curve solutions of AW CrB.

Parameters	unspotted	spotted
$g_1 = g_2$	0.32	0.32
$A_1 = A_2$	0.5	0.5
$x_{1bol} = x_{2bol}$	0.659	0.659
$y_{1bol} = y_{2bol}$	0.178	0.175
$x_{1V} = x_{2V}$	0.701	0.701
$y_{1V} = y_{2V}$	0.285	0.285
$x_{1R} = x_{2R}$	0.607	0.607
$y_{1R} = y_{2R}$	0.286	0.286
$x_{1I} = x_{2I}$	0.517	0.517
$y_{1I} = y_{2I}$	0.270	0.270
T_1	6700 K	6700 K
T_2	6769(11) K	6808(10) K
$q = m_2/m_1$	0.0992(4)	0.1012(4)
i	81.°6(3)	82.°1(1)
$\Omega_1 = \Omega_2$	1.908(2)	1.913(2)
f	75%(3)	75%(3)
$L_1/(L_1+L_2)_V$	0.87(1)	0.87(1)
$L_1/(L_1+L_2)_R$	0.90(1)	0.90(1)
$L_1/(L_1+L_2)_I$	0.92(1)	0.92(1)
Spot parameters		
ϕ		114°
θ		290°
r_s		21°
$T_s/T_\star$		0.96
χ^2	0.129	0.104

contact angle diagram plotted in their fig. 3 can be used as a consistency check on the solution found by the WD method. By estimating the internal contact angle from the light curve, and by using the inclination found by the WD method, a mass-ratio $q \sim 0.11$ is estimated from this diagram. This is in good agreement with the solution found by the WD model. A significant difference would indicate third light or another complication.

5 RESULTS AND CONCLUSION

The light curves obtained by CCD photometric observations in the V, R_c, and I_c passbands were analysed simultaneously with the WD method, as implemented in PHOEBE. Since AW CrB shows total eclipses the photometric parameters can be determined reliably. The photometric solutions suggest that AW CrB is an extreme low mass-ratio overcontact binary with $q = 0.10$ and a high degree of overcontact $f = 75\% \pm 3$. This places AW CrB among the few contact binaries with the lowest mass-ratios known up to now. The mass-ratio of the components, which is related to the angular momentum loss and mass transfer, is one of the crucial parameters in the evolution of close binary systems. Table 6 lists the currently known contact binaries with mass-ratios $q \lesssim 0.12$.

Table 7. Periods and period change rates for low mass-ratio overcontact binaries.

Star	Period $(days)$	$\mathrm{d}P/\mathrm{d}t$ $(d\ yr^{-1})$	P_c (yr)	Ref.[c]
V857 Her	0.38223	$+2.90 \times 10^{-7}$		(1)
SX Crv	0.31660	-1.05×10^{-6}		(2)
V870 Ara	0.39972			(3)
FP Boo	0.64048			(4)
DN Boo	0.44757			(5)
V1191 Cyg	0.31338	$+1.3 \times 10^{-6}$		(6)
CK Boo	0.35515	$+3.54 \times 10^{-7}$	15.8[a]	(7)
FG Hya	0.32783	-1.96×10^{-7}	36.4[a]	(8)
GR Vir	0.34698	-4.21×10^{-7}	19.3[b]	(9)
ϵ CrA	0.59143	$+4.67 \times 10^{-7}$		(10)
AW UMa	0.43873	-2.94×10^{-8}	17.6[b]	(11)

[a] Cyclic period change attributed to magnetic activity cycles
[b] Periodic period change attributed to the presence of a third body
[c] References: same as in Table 6

The light curves displayed in Figure 1 suggest that AW CrB is an A-type overcontact binary system according to the classification of Binnendijk (1970). However, we derived a secondary temperature of $T_{\rm eff} = 6808 \pm 10\ K$, which is higher than that of the primary component. A weak O'Connell effect is observed with Max I slightly fainter than Max II. The position of AW CrB coincides furthermore with the *ROSAT* X-ray source 1RXS J161520.0+354218 (Geske, Gettel & McKay 2006) indicating enhanced chromospheric and coronal activity. The O'Connell effect may be explained by a model with a cool starspot on the primary component. The best model is obtained with a cool spot on star 1, with $T_s/T_\star = 0.96$, spot radius $r_s = 21°$, colatitude $\phi = 114°$, and longitude $\theta = 290°$.

The evolutionary status of the primary component can be inferred from its mean density (Mochnacki 1981, 1984, 1985). Without knowledge of the absolute dimensions the mean density $\overline{\rho_1}$, $\overline{\rho_2}$ of each component can be calculated with the formulae,

$$\overline{\rho_1} = \frac{0.079}{V_1(1+q)P^2}\ g\ cm^{-3},\ \overline{\rho_2} = \frac{0.079q}{V_2(1+q)P^2}\ g\ cm^{-3}, \quad (5)$$

where $V_{1,2}$ are the volumes of the components using the separation A as the unit of length, q is the mass-ratio and P the period in days. For AW CrB the mean densities $\overline{\rho_1}$, $\overline{\rho_2}$ can be determined to be 0.60 and 1.03, respectively. In the traditional contact binary models, energy transfer from the primary to the secondary is assumed to explain the nearly equal temperatures of both components despite their considerable different masses. Following Mochnacki (1981), the colour of the primary can be corrected for this energy transfer in order to compare the density of the primary with that of a zero-age main sequence star of the same spectral type. For AW CrB the corrected colour index $(B-V)_1 = 0.38$. Figure 6 shows the position of the primary component of AW CrB in the $(B-V)_1$ - mean density diagram together with the primaries of other contact binaries. The mean den-

Table 6. Physical parameters for contact binaries with the lowest known mass-ratios.

Star	Type	M_1 ($M_\odot$)	M_2 ($M_\odot$)	R_1 ($R_\odot$)	R_2 ($R_\odot$)	L_1 ($L_\odot$)	L_2 ($L_\odot$)	T_1 (K)	T_2 (K)	q	f %	Ref.[c]
V857 Her[a]	A							8300	8513	0.0653	84	(1)
SX Crv	A	1.246	0.098	1.347	0.409	2.590	0.213	6340	6160	0.0787	27	(2)
V870 Ara	W	1.503	0.123	1.670	0.610	2.960	0.500	5860	6210	0.082	96	(3)
FP Boo	A	1.614	0.154	2.310	0.774	11.193	0.920	6980	6456	0.096	38	(4)
DN Boo	A	1.428	0.148	1.710	0.670	3.750	0.560	6095	6071	0.103	64	(5)
V1191 Cyg	A*	1.29	0.13	1.31	0.52	2.71	0.46	6500	6610	0.105	74	(6)
CK Boo	A	1.442	0.155	1.521	0.561	2.924	0.401	6150	6163	0.106	91	(7)
FG Hya	A*	1.444	0.161	1.405	0.591	2.158	0.412	5900	6012	0.112	86	(8)
GR Vir	A*	1.376	0.168	1.490	0.550	2.806	0.493	6300	6163	0.122	78	(9)
ϵ CrA	A	1.70	0.23	2.10	0.85	7.75	1.02	6678	6341	0.127	25	(10)
AW UMa[b]	A	1.79	0.14	1.88	0.66	8.26	0.92	7175	7110	0.08	80	(11)

* Alternations between the A and W types have been reported for these stars.
[a] For V857 Her no spectroscopic mass-ratio could be determined yet. Pribulla et al. (2009) found a contribution from a early-type component in their spectra and note that the shallownes of the eclipses might be caused by the 3rd light of this additional component and therefore put in doubt the low mass-ratio obtained by light curve modelling.
[b] Pribulla & Rucinski (2008b) found a spectroscopic mass-ratio of $q \simeq 0.10$ and found strong indications that the system is not a contact binary.
[c] References: (1) Qian et al. (2005b); (2) Szola et al. (2004); (3) Szalai et al. (2009); (4) Gazeas et al. (2006); (5) Şenavcı et al. (2008); (6) Ulas et al. (2012); (7) Kalci & Derman (2005); (8) Qian & Yang (2005a); (9) Qian & Yang (2004); (10) Yang et al. (2005); (11) Yang (2008)

sities of the other primaries are calculated from data taken from Pribulla, Kreiner & Tremko (2003). Contact binaries with components in poor thermal contact and hot contact binaries, indicated respectively as type B and E in the catalogue, have been excluded. The zero-age main sequence and terminal-age main sequence lines have been taken from Mochnacki's (1981) Fig. 3. The diagram indicates that the primary component of AW CrB has already moved away from the ZAMS. This is the case for the majority of A-type contact binaries. The secondary's mean density $\overline{\rho_2} = 1.03$ is nearly equal to the density of a ZAMS star of the same spectral type. The evolutionary status of the secondary is however more difficult to judge as some of its properties, including the radius and thus the mean density, are possibly influenced by the energy transfer from the primary (Yang & Liu 2001). In order to compare the evolutionary status of the primary components in A-type low mass-ratio contact binaries, the mean densities of the primaries for the stars listed in table 6 are plotted in Figure 6 with a filled triangle. There is no indication that these primaries are evolved in a greater or lesser extent than the primaries of A-type stars with a higher mass-ratio. For the W-type contact binaries, the primaries of the systems with a mass-ratio $q \lesssim 0.21$ have been plotted with filled circles. The diagram suggests that these are more evolved than the W-type members with a higher mass-ratio. CV Cygni's primary has a very low mean density, which is also supported by its F8III spectral type. It should be noted however, that the Binnendijk classification of this star is uncertain (Vinkó, Hegedüs & Hendry 1996).

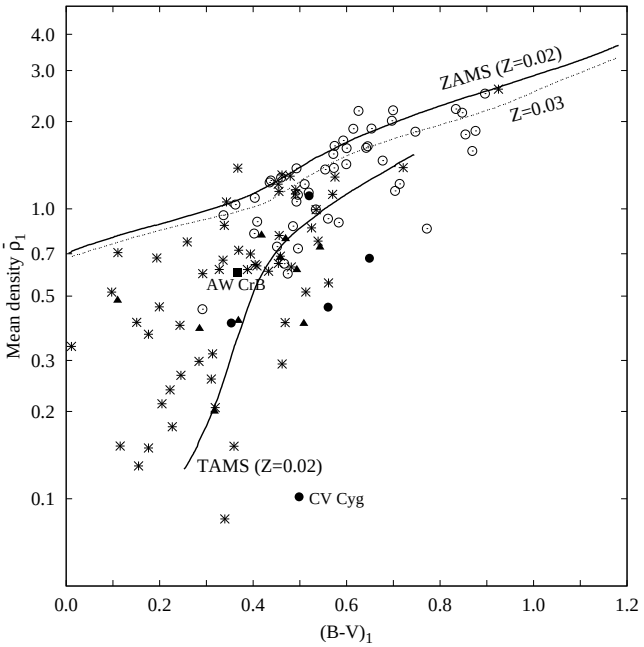

Figure 6. Corrected colour - mean density diagram for W-type (open circles) and A-type (crosses) primaries. The low mass-ratio W-type and A-type primaries are plotted with filled circles and filled triangles respectively. AW CrB is indicated with a filled square. The zero-age main sequence and terminal-age sequence lines are taken from Mochnacki's (1981) Fig. 3.

The orbital period analysis based on observations collected from public available data of the NSVS and WASP project, the Jin et al. (2003) paper, and the present paper, reveal an increasing period for AW CrB. The form of this period change is unclear. Additional timings of minimum light over a longer time span are required to be conclusive. A sudden period increase of $\Delta P = 2.3 \times 10^{-6} days$ or 0.2 s may have occurred around $2005 - 2007$. However, continuous period variations are commonly encountered in contact binaries and are more acceptable. Table 7 lists the period change rates for a number of extreme mass-ratio

contact binaries. In case of a continuously increasing period, the period change rate for AW CrB is estimated to be $\mathrm{d}P/\mathrm{d}t = 3.58 \times 10^{-7}\ d\ yr^{-1}$ or $0.03\ s\ yr^{-1}$. Such a period change is usually attributed to mass transfer. If a mass of 1.4 $M_\odot$ is assumed for the primary component based on the colour indices, then a conservative mass transfer rate from the less massive to the more massive component is estimated to be $5.1 \times 10^{-8}\,M_\odot\ yr^{-1}$. With mass transferring, the orbital angular momentum decreases while the spin angular momentum increases. When the spin angular momentum of the system is more than a third of its orbital angular momentum, this kind of low mass-ratio binaries with a high degree of overcontact may evolve into a rapidly rotating single star (Hut 1980).

Due to the short time span of the observations, about 12 year or only 12000 orbital revolutions, a cyclic period variation cannot be ruled out. Periodic variations, sometimes superimposed on a secular period change, have been reported for several W UMa-type stars. These periodic variations are usually explained by a light-time effect via the presence of a third body, e.g. GR Vir (Qian & Yang 2004) and XY Leo (Yakut et al. 2003) among other stars. Pribulla & Rucinski (2008a) argue that perhaps all cool contact binaries are members of multiple systems, supporting the theory that Kozai cycles accompanied by the tidal friction may play an important role in close binary formation (Stępień 2011, and references therein). In case period variations are not strictly periodic, they are usually explained by magnetic activity cycles in both components, e.g. FG Hya (Qian & Yang 2005a) and CK Boo (Kalci & Derman 2005). The W UMa stars are fast-rotating solar-type stars and are known to show enhanced chromospheric and coronal activity. Applegate (1992) and Lanza et al. (1998) proposed that the orbital period changes in close binaries are a consequence of magnetic activity in one or both of the component stars.

Since the period variation of AW CrB is very important to understand its evolutionary state, it needs further long-term photometric monitoring for accurate epochs of light minimum. In order to obtain the absolute parameters of AW CrB, and to check the derived photometric mass-ratio, spectroscopic observations are required.

ACKNOWLEDGEMENTS

I gratefully acknowledge the AAVSO and the Curry Foundation for providing the CCD camera on loan. I thank Patrick Wils for proofreading the draft of this paper and the referee, Professor S. W. Mochnacki, for suggesting several improvements to the paper. This study used data from the NSVS created jointly by the Los Alamos National Laboratory and the University of Michigan, and funded by the US Department of Energy, the National Aeronautics and Space Administration (NASA) and the National Science Foundation (NSF). This research also used data from the WASP public archive. The WASP consortium comprises of the University of Cambridge, Keele University, University of Leicester, The Open University, The Queen's University Belfast, St. Andrews University and the Isaac Newton Group. Funding for WASP comes from the consortium universities and from the UK's Science and Technology Facilities Council. Additionally this study made use of NASA's Astrophysics Data System, and the SIMBAD and VizieR databases operated at the CDS, Strasbourg, France.

REFERENCES

Akerlof C. et al., 2000, AJ, 119, 1901
Applegate J.H., 1992, ApJ 385, 621
Binnendijk L., 1970, Vistas in Astron., 12, 217
Butters O.W. et al., 2010, A&A, 520, L10
Cox A.N., 2000, Allens Astrophysical Quantities, 4th ed., New York, NY: AIP Press, Springer
Gazeas K.D., Niarchos P.G., Zola S., Kreiner J.M., Rucinski S.M. 2006, AcA, 56, 127
Geske M.T., Gettel S.J., McKay T.A., 2006, AJ, 131, 633
Henden A. et al., 2012, in prep.
Howell S.B., Warnock A.I., Mitchell K.J. 1988, AJ, 95, 247.
Hut P., 1980, A&A, 92, 167
Jester S. et al., 2005, AJ, 130, 873
Jin H., Kim S.-L., Kwon S.-G., Youn J.-H., Lee C.-U., Lee D.-J., Kim K.-S., 2003, A&A, 404, 621
Kalci R., Derman E., Astron. Nachr., 2005, 326, 342
Kwee K.K., van Woerden H., 1956, Bulletin of the Astronomical Institutes of the Netherlands, 12, 327
Lanza A.F., Rodonó M., Rosner R., 1998, MNRAS, 296, 893
Lucy L.B., 1967, Zeitschrift fuer Astrophysik, 65, 89
Maceroni C., van't Veer F., 1993, A&A, 277, 515
Mochnacki S.W., Doughty N.A., 1972, MNRAS, 156, 51
Mochnacki S.W., 1981, ApJ, 245, 650
Mochnacki S.W., 1984, ApJS, 55, 551
Mochnacki S.W., 1985, ApJS, 59, 445
Prša A., Zwitter T., 2005, ApJ, 628, 426
Pribulla T., Kreiner J.M., Tremko J., 2003, CoSka, 33, 38
Pribulla T., Rucinski S.M., 2008a, ESO Astrophysics Symposia, Springer-Verlag Berlin Heidelberg, 163
Pribulla T., Rucinski S.M., 2008b, MNRAS, 386, 377
Pribulla T. et al., 2009, AJ, 137, 3655
Qian S.-B., Yang Y.-G., 2004, AJ, 128, 2430
Qian S.-B., Yang Y.-G., 2005a, MNRAS, 356, 765
Qian S.-B., Zhu L.-Y., Soonthornthum B., Yuan J.-Z, Yang Y.-G., He J.-J., 2005b, MNRAS, 130, 1206
Rasio F.A., 1995, ApJ, 444, L41
Rucinski S.M., 1969, Acta Astron. 19, 245
Şenavcı H.V., Nelson R.H., Özavcı İ., Selam S.O., Albayrak B., 2008, NewA, 13, 468
Stępień K., 2006, AcA, 56, 199
Stępień K., 2011, AcA, 61, 139
Szalai T., Kiss L.L., Mészáros S., Vinkó J., Csizmadia S., 2007, A&A, 465, 952
Szola S., 204, AcA, 54, 299
Terrell D., Wilson R.E., 2005, Ap&SS, 296, 221
Terrell D., Gross J., Cooney W.R. Jr, 2012, AJ, 143, 99
Tylenda R. et al., 2011, A&A, 528, A114
Ulaş B., Kalomeni B., Keskin V., Köse O., Yakut K., 2012, New Astronomy, 17, 46
van Hamme W., 1993, AJ, 106, 2096
Vinkó, J., Hegedüs, T., Hendry, P.D., 1996, MNRAS, 280, 489
Wilson R.E., Devinney R.J., 1971, ApJ, 166, 605
Wilson R.E., Devinney R.J., 1972, ApJ, 171, 413
Wilson R.E., 1979, ApJ, 234, 1054

Wilson R.E., 1994, PASP, 106, 921
Wozniak P.R. et al., 2004, AJ, 127, 2436
Yakut K., Ibanoglu C., Kalomeni B., Degirmenci Ö.L., 2003, A&A, 401, 1095
Yang Y., Liu Q., 2001, AJ, 2001, 122, 425
Yang Y.-G., Qian S.-B., Zhu L.-Y., He J.-J., Yuan J.-Z, 2005, PASJ, 57, 983
Yang Y., 2008, Ap&SS, 2008, 314, 151